Initial Response of Nightside Auroral Currents to a Sudden Commencement: Observations of Electrojet and Substorm Onset

Yun-Liang Zhou[1] ![ORCID] and **Hermann Lühr[2]** ![ORCID]

[1]Department of Space Physics, School of Electronic Information, Wuhan University, Wuhan, China, [2]GFZ German Research Centre for Geosciences, Section 2.3, Geomagnetism, Potsdam, Germany

Abstract Storm sudden commencements (SSC) often precede geomagnetic storms. Commonly, it takes some hours from the step-like change that marks the SSC to the start of the magnetic storm activity. In a subset of cases, however, auroral activity starts almost instantaneously after the SSC. To the authors knowledge, the conditions that enable this rapid activation have not been investigated in detail before. Here we consider all the sudden commencements (SC) during the years 2000–2020. Our focus is on the initial response of the auroral currents on the nightside. For that purpose, we make use of the IMAGE Magnetometer Network in Fennoscandia. In about 30% of SC events an initial activation of the westward electrojet is observed. Magnetic deflections of the northward component, surpassing frequently 1,000 nT, are observed only 4 min after the SC. These intense westward currents, flowing typically in narrow channels of 1°–2° latitudinal width, last some 10 min. The electrojets are conjugate to regions in the magnetosphere near geostationary orbits. In several cases geomagnetic substorm onsets are observed about 30 min after the SC. These start typically at fairly high latitude, around 71° magnetic latitude. This is an indication for rather quiet conditions preceding the onset. The magnetic pulse of the SC seems to play an important role in initiating the strong electrojets and the substorms. These initial activities are of relevance for space weather effects because of their strong and rapid variations. This paper provides detailed observations of the initial auroral activity following some SCs.

1. Introduction

A step-like increase in solar wind dynamic pressure generally causes, when passing by Earth, a steep increase in the horizontal component of the geomagnetic field. This increase is called sudden commencement (SC). Traditionally, SCs are detected by ground-based magnetometers at low and middle latitudes. In many cases a geomagnetic storm follows within hours after the solar wind pressure pulse passage. Then the rapid field strength increase is termed storm sudden commencement (SSC). This steep rise of the horizontal component preceding many magnetic storms was already recognized about 100 years ago (Chapman, 1929). A more detailed analysis of the geomagnetic field response to sudden solar wind pressure changes, however, were only possible after globally distributed magnetic observatories were available, in particular after the International Geophysical Year (IGY) 1957–1958. Comprehensive studies have been performed by for example, Araki (1977, 1994); Petrinec et al. (1996); Engebretsen et al. (1999). All these studies and related references focused on the phenomena confined primarily to the dayside.

Although the above studies have advanced significantly our understanding of SCs, several open questions are left. Lühr et al. (2009) investigated SCs on the nightside by comparing ground-based observations with CHAMP satellite data. At low and middle latitudes both systems recorded quite similar variation of the horizontal field component. This implies that at those latitudes ionospheric currents do not contribute to the SC signature during the dark hours. Another important finding was that the SC amplitude increased poleward of about 40° latitude, also synchronously above and below the ionosphere. The authors interpret this as a far-field effect of field-aligned currents (FACs) connecting to auroral latitudes.

To the authors knowledge there are hardly any studies investigating systematically the SC effects on the auroral current systems on the night side. As mentioned above, SCs precede often magnetic storms. In many cases the main phase of the storm starts some hours after the SSC. But there are also numerous cases where intense magnetic activity starts right after the SSC. These events are at the focus of this study.

The Ebro Observatory in Spain maintains a list of SC events. Since 2006 their website classifies the SCs in three types of events: SSC for which "an increase of magnetic activity within the next 48 hr" is observed, or Sudden Impulse (SI) if no storm signature is detected at middle latitudes, and also Solar Flare Effect (SFE). As SFEs do not cause significant magnetic effects at auroral latitudes on the nightside, these events were discarded here. Most of our studied events are from the year before 2006, without classification. Thus, we make use in the following of the paper of the naming convention SC, in order to avoid the ambiguity between SI and SSC.

Here we make primarily use of recordings by the instruments of the IMAGE Magnetometer Network in Fennoscandia. Those stations are well suited to monitor the auroral activity with good spatial and temporal resolution. The high-latitude data are supplemented by measurements from magnetic observatories from middle latitudes. As study period we chose the last two solar cycles.

In the sections to follow we first describe the data sources and data used in the study. Then we present in Section 3.1 a number of representative examples exhibiting clear auroral activity immediately following the SC. In Section 3.2 statistical properties of all the SCs and in particular those of our considered SCs are presented. Here also the relations to solar wind and interplanetary magnetic field (IMF) are considered. In the discussion section we try to interpret the observations and compare them with results from earlier studies. Generally, this paper focuses on the observational features related to initial auroral activity following directly SCs. An assessment of possible mechanisms in the magnetosphere, responsible for the rapid auroral response, will be discussed in a follow-up study.

2. Datasets and Processing Approach

For this study, times of SC occurrences are of interest. For identifying the events we made use of the SC list that is maintained by the group of the Ebro Observatory in Spain. A rather complete list of events for the past decades is accessible through their web site http://www.obsebre.es/en/rapid. Here we considered all the listed events during the years 2000 through 2020. For these two decades there is a good coverage of supporting satellite data, which may be considered at a later stage for interpreting the observed phenomena.

The response of high-latitude current systems to an SC is studied with the help of recordings from the IMAGE magnetometer network (Lühr et al., 1998; Viljanen & Häkkinen, 1997). The observation sites are located in the Fenno-Scandian sector and cover all the latitudes from subauroral to polar cap regions. The magnetic local time (MLT) in that sector is about 2 hr ahead of the Universal Time (UT): MLT $\cong$ UT + 2 hr. For more details of the magnetic array see: https://space.fmi.fi/image/www/index.php?page=home. The magnetic field readings of the relevant stations have been downloaded from the web site: https://space.fmi.fi/image/www/index.php?page=user_defined.

Since the focus of this study is on nightside phenomena, only SC events occurring during the hours 18:00–03:59 UT are considered, which cover the time span when the IMAGE stations are connected to the magnetospheric night sector.

For the interpretation also the SC-related auroral current systems and magnetic field recordings at middle latitudes are considered. These are located in the European-African sector. In detail these are Brorfelde (BFE, 55.63 N, 11.67°E), Niemegk (NGK, 52.07°N, 11.68°E), Fürstenfeldbruck (FUR, 48.17°N, 11.28°E), L'Aquila (AQU, 42.38°N, 13.32°E), Hermanus (HER, 34.43°S, 19.23°E), Tamanrasset (TAM, 22.79°N, 5.53°E), and Honolulu (HON, 21.32°N, 202°E) as a dayside SC reference. During the later years no more data were available from the stations BFE and AQU. These are substituted by Tartu (TAR, 58.26°N, 26.46°E) and Duronia (DUR, 41.65°N, 14.47°E), respectively. For all these magnetic observatories 1 min average data were retrieved from the INTERMAGNET web site: https://www.intermagnet.org/data-donnee/download-eng.php#view.

3. Observations

Commonly the SC is regarded as a precursor for a magnetic storm. The main magnetic activity, however, starts generally only order of hours later. But in some cases, there is no delay. Here we are interested in events where significant auroral currents (electrojets) on the nightside start flowing right after the SC, within minutes. There
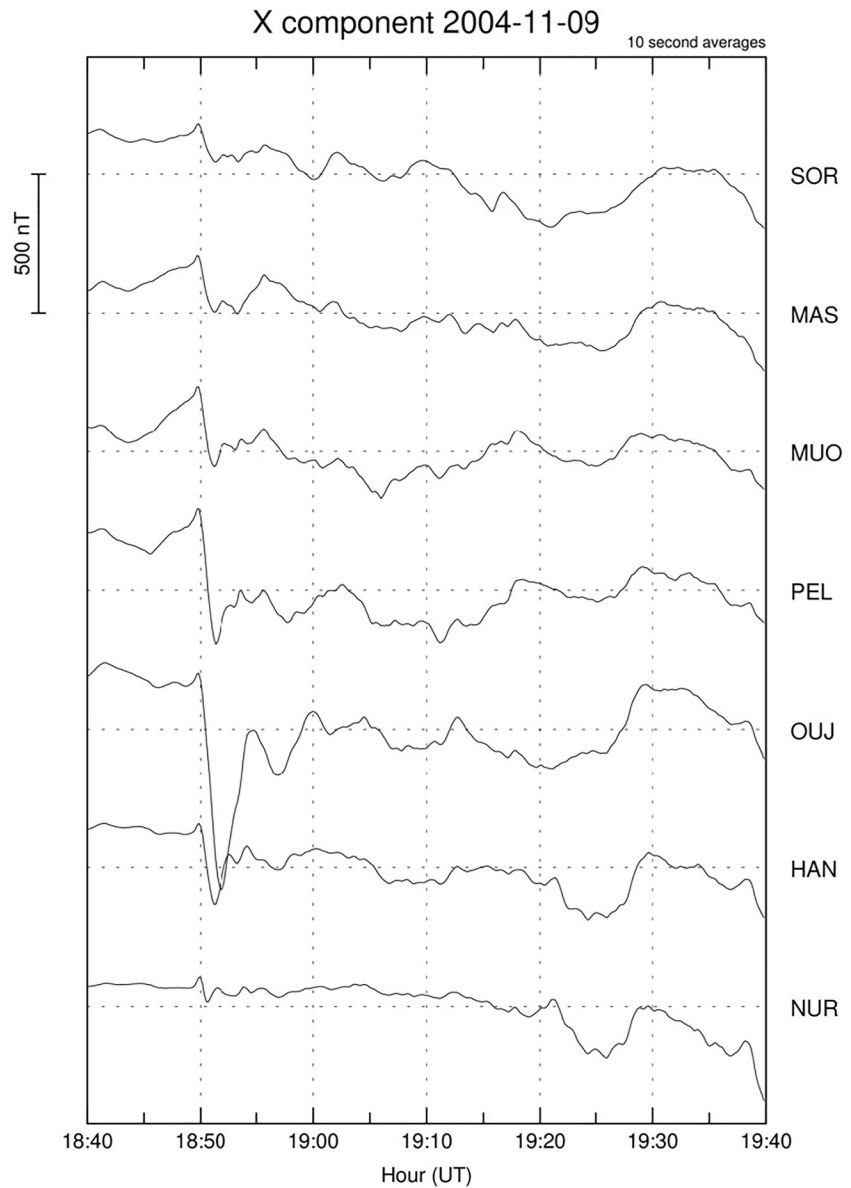
Figure 1. Example of an intense and short-lived auroral westward electrojet starting immediately after the sudden commencement at 18:49 Universal Time (UT).

are two types of events. The more prominent start with a rapid negative deflection, reaching partly more than 1,000 nT in typically 4 min after the SC. In other cases, a substorm onset occurs within about 30 min after the SC. Before discussing the characteristic properties of these events, we will first present a few representative examples for visualizing the details.

3.1. Examples

A good example for a rapid activation has been observed on 09-11-2004 in the pre-midnight sector. Here a rather short-lived (~5 min) negative deflection of the northward, X component at Oulujärvi (OUJ) followed the SC at 18:49 UT. The peak amplitude reached −870 nT at 18:52 UT, see Figure 1. This negative spike is well confined in latitude. At neighboring stations the negative peaks occurred slightly earlier than at OUJ. That implies, the
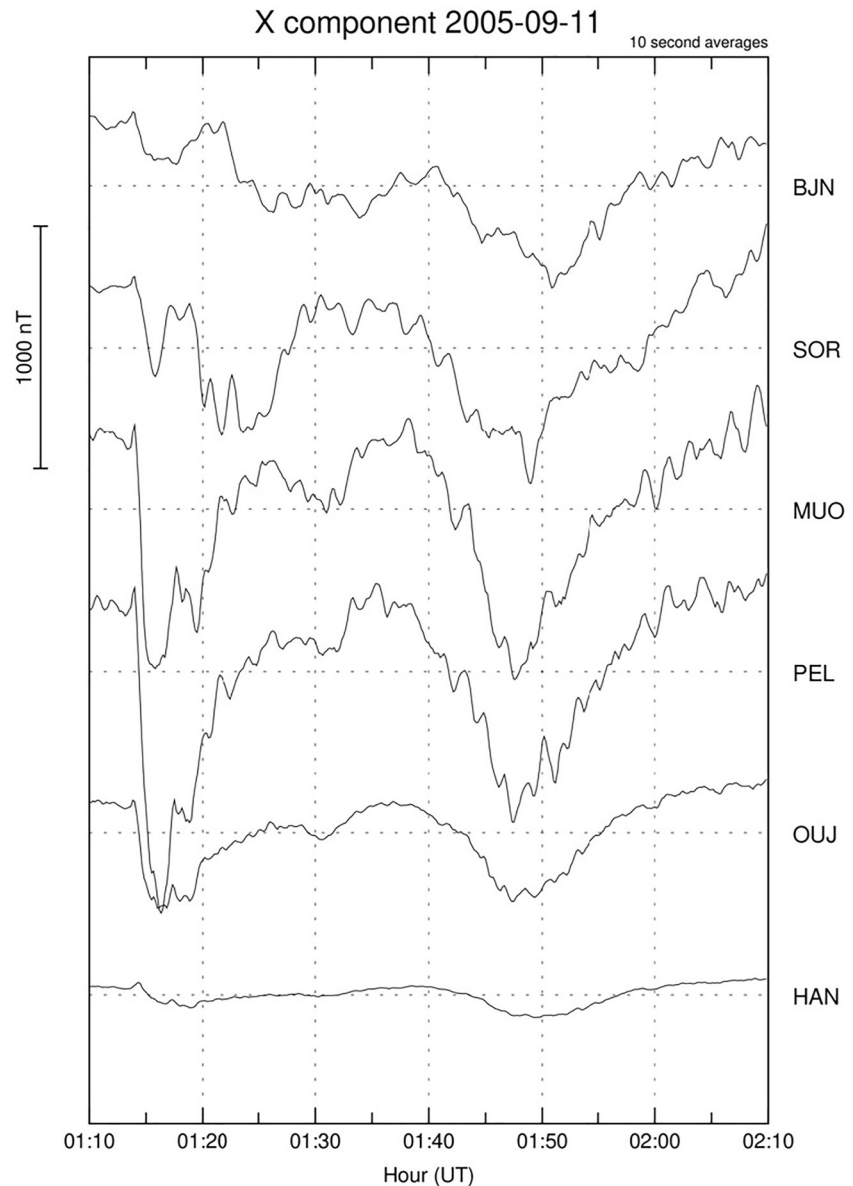
Figure 2. Similar example as in Figure 1, but for the sudden commencement at 01:13 Universal Time (UT).

current channel got narrower when intensifying. After the decay of the intense westward current only moderate activity followed for the next 30 min.

A rather similar event was observed on 11-09-2005 in the early morning sector. Right after the SC (short positive spike at 01:13 UT) the X component drops at Pello (PEL) by more than 1,000 nT within a minute and reaches its negative peak at 01:16 UT, see Figure 2. The signal lasts for about 5 min before it gradually returns to pre-event level. The current signature comprises obviously two successive peaks. The first appears almost simultaneously at the different latitudes, while the second follows successively later at higher latitudes. About half an hour later another activation is observed, but that is not further considered here.

A more common activation signature appears on 31-03-2001 in the early morning sector. Right after the SC (small positive spike at 00:52 UT) the X component drops off. In PEL it goes down by about 1,300 nT and stays there for about 10 min, see Figure 3. A second activation occurs 10 min later, exhibiting comparable deflections further north (Sørøya, SOR). Thereafter, the activity gradually fades away.
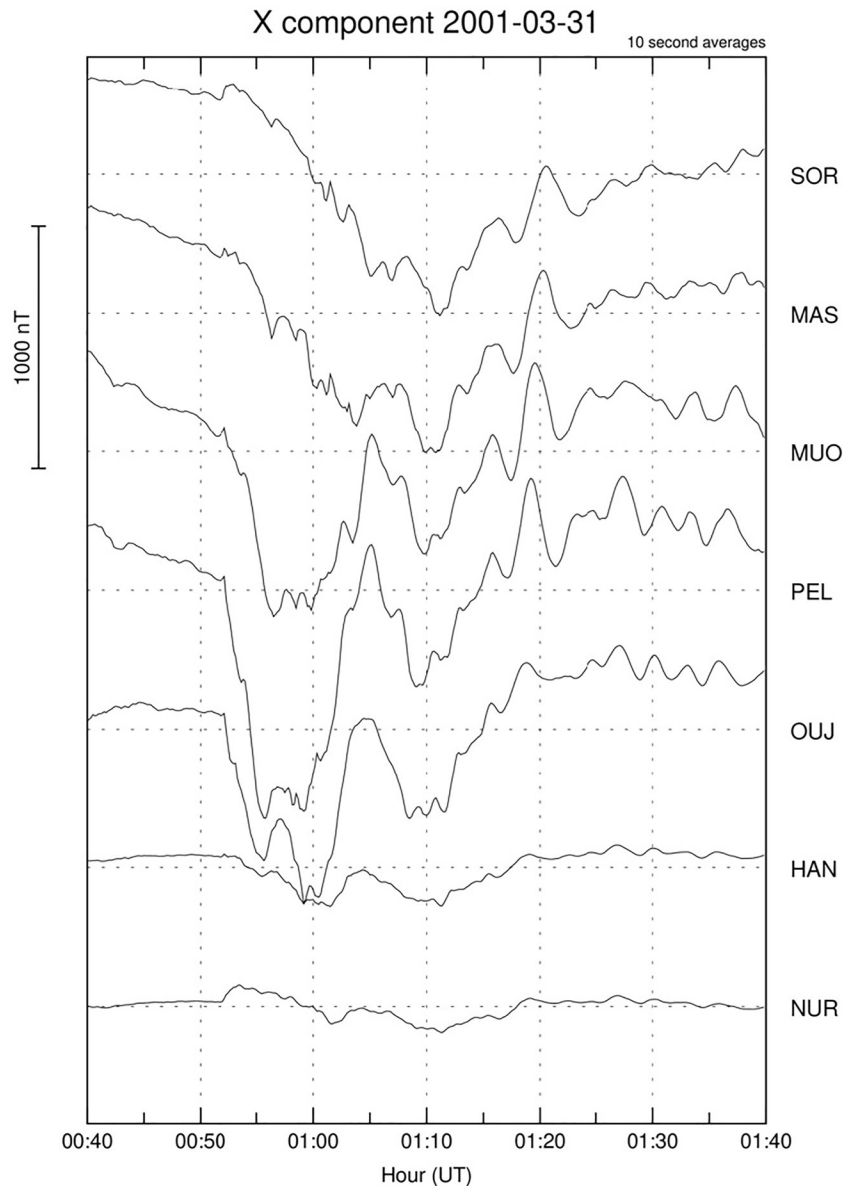
Figure 3. A similar initial activation as the events shown before, following the sudden commencement at 00:52 Universal Time (UT). Here the electrojet lasted for about 10 min, and a second activation followed 10 min later.

In other cases, substorm onsets are observed soon after the SC. A good example occurs on 18-05-2002 shortly before midnight. A sharp decrease of the X component at Bear Island (BJN) at 20:16 UT (8 min after SSC) marks the onset, see Figure 4. During the subsequent 40 min the activity propagates further southward and increases. A confirmation for the substorm-type of activity comes from the mid-latitude recordings (Figure 4, right column). The northward (Bx) components at all those observatories show positive deflections, and they vary in phase, while in case of the By components the southern hemisphere observatory, HER, exhibits an anti-phase variation with respect to the northern counterparts. All this is consistent with the typical mid-latitude signature of a substorm current wedge. In the discussion section this substorm-related signature will be treated in more details.

There are also cases where both types, rapid decrease of X component and substorm onset are observed to follow each other. One such event occurred on 07-09-2017 shortly after midnight, see Figure 5. Immediately following the SC at 23:00 UT, the X component at OUJ dropped down by about 1,600 nT within minutes and stayed there for some 5 min. Amplitudes at neighboring stations are much smaller, implying again an intense westward current
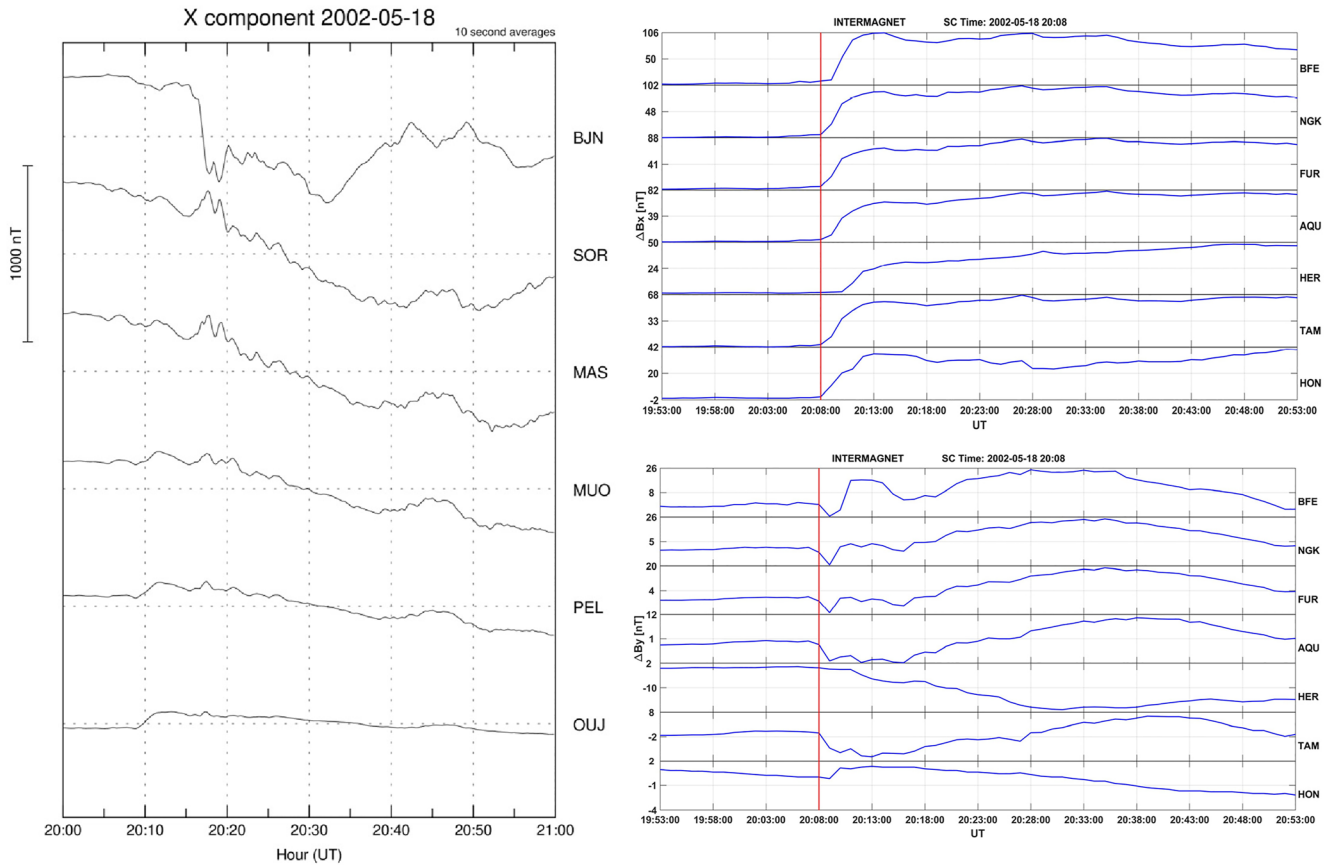
Figure 4. Onset of a substorm near BJN soon after the sudden commencement (SC) at 20:08 Universal Time (UT). Confirmation for the substorm comes from mid-latitude observatories. The *By* component at HER varies in a direction opposite to the northern hemisphere recordings.

channel, narrow in latitude. It is followed by a second negative deflection at higher latitude stations about 10 min later. Around 23:18 UT, the decreases of the *X* components at BJN and SOR mark the onset of a substorm with a typical longer lasting negative bay. This interpretation is also supported by mid-latitude magnetic recordings. Again, we find an anti-phase variation of *By* at HER that starts synchronously with the onset marked at high latitudes. This event shows that the two types of magnetic activity, following directly the SC, do not inhibit each other.

3.2. Statistical Properties of SC Events

For our analysis we made use of the past 21 years, which are reasonably well accompanied by low-Earth orbiting (LEO) satellites. This period covers practically the last two solar cycles, 23 and 24. In total 347 SC events have been reported. Over the years the occurrence frequency of SCs follows closely the variation of the solar activity. Peak counts have been reported for the years 2001 and 2014. Smallest numbers were found in 2008 and 2020. When combining all the years, there is no significant seasonal variation observed. However, when looking at the diurnal variation a clear UT dependence emerges. Higher SC occurrence rates are recorded between 06 and 18 UT, when the European and American continents are in daylight. During the other hours significantly lower counts are reported. The diurnal variation of SC occurrence rate can reasonably well be approximated by a sine curve, see Figure 6. This curve reaches its peak at 12 UT, and shows a reduced occurrence around UT-midnight, amounting only to 66% of the rate at 12 UT. This is in the first place surprising because processes on the sun are not dependent on the time on Earth. For an explanation it may be assumed that SCs are better detectable on the dayside. Thus, a considerable number of events seem to be missed when the Pacific sector is on the dayside, probably due to a sparser station coverage compared to the European-American sector.
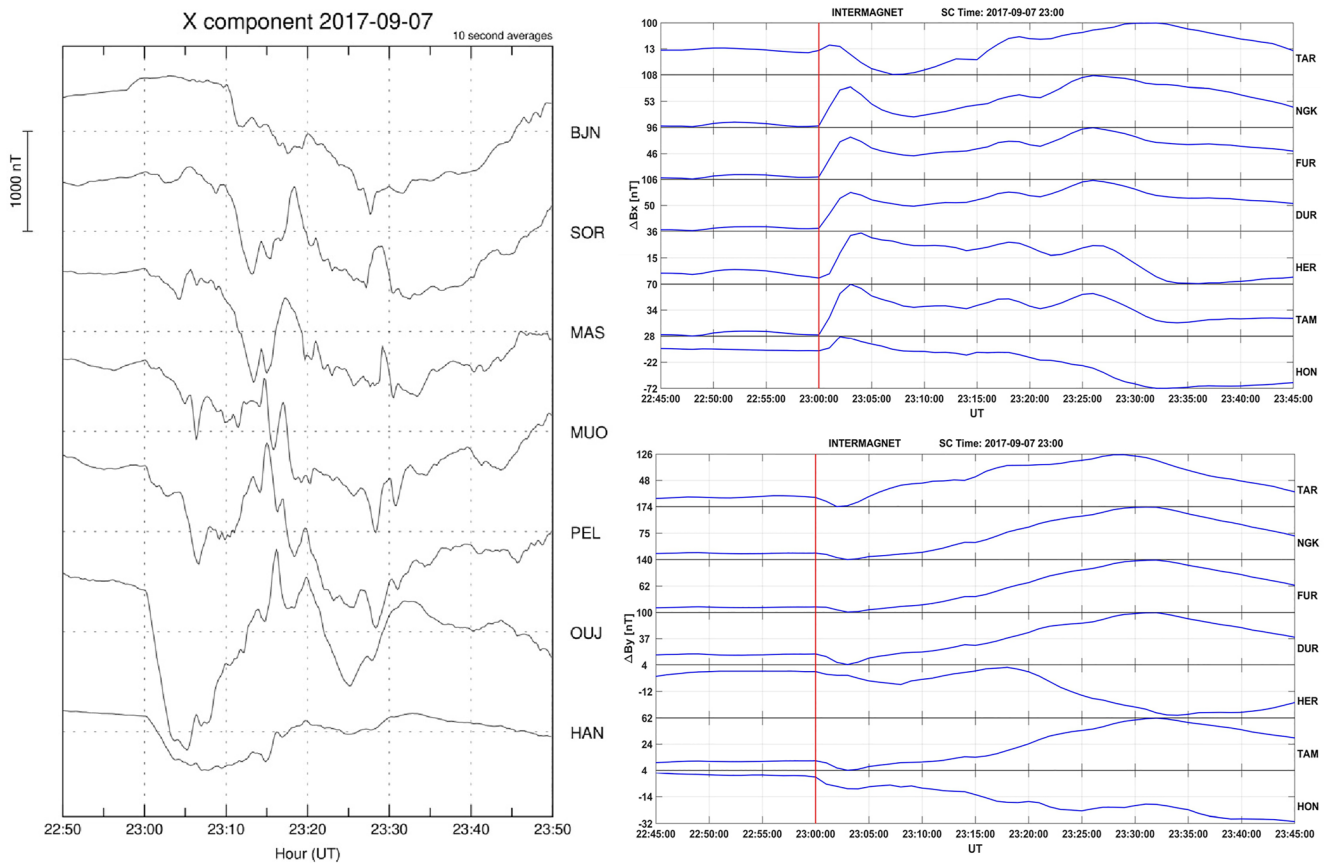
Figure 5. Another example of an early substorm onset around 23:18 Universal Time (UT) after the sudden commencement (SC) at 23:00 UT. In addition to that an intense electrojet is also observed right after the SC.
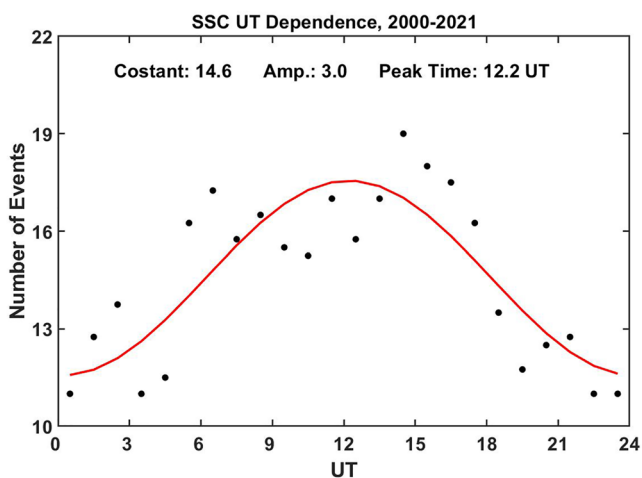

Figure 6. Variation of detected sudden commencements (SC) occurrence frequency vs. Universal Time (UT). Clearly more SCs are detected around 12 UT than 24 UT.

In this study we consider only SCs during 18:00–03:59 UT, the 10 night-hours in Scandinavia. For those hours 123 events were identified. This number is smaller than expected for the part of the total SC number that occur during 10 hr of a day. Reason for that is the above-mentioned reduced detection rate around UT night-hours. In a next step we visually inspected all these events and picked those, which exhibit considerable auroral activity of at least 200 nT within about half an hour after the SC. Overall, 31 active events were selected for further study. The times of these SC events are listed in Tables 1 and 2. A table containing all the 92 quiet nighttime SC events is included in Supporting Information S1.

Table 1 contains the 20 SC events which are immediately followed by significant electrojet activity. In the fifth column the peak negative deflections of the X component are listed, and the right-side column gives the approximate L-value of the peak deflection. There is a tendency observed that larger deflections occur preferably at lower latitudes. But there is no one-to-one relation between amplitude and latitude. Generally, the peak-amplitude locations are conjugate to magnetospheric regions near geostationary distances.

Table 2 lists the 19 events, at which a substorm started within about 30 min after the SC. The sum of events from both tables clearly surmounts the number of our 31 active events. That means, in 8 cases the initial electrojet after the SC was followed later by a substorm. The event, which show both

Table 1
List of Events That Exhibit Intense Auroral Electrojets Starting Immediately After the SC

Year	Month	Day	UT	Peak deflect	Peak time	Total current	Peak density	Mlat	Half-width	L-Value
2000	2	11	23:52	−610 nT	23:56	1.19 MA	1.36 A/m	64.34°	278 km	5.9
2000	10	3	00:53	−220 nT	00:58	0.19 MA	1.09 A/m	62.51°	56 km	5.2
2001	3	27 *	01:44	−200 nT	01:49	0.21 MA	0.65 A/m	66.32°	101 km	6.8
2001	3	31	00:52	−1,320 nT	00:56	1.11 MA	6.17 A/m	62.69°	57 km	5.2
2001	4	18*	00:46	−570 nT	00:50	0.54 MA	2.20 A/m	63.38°	79 km	5.5
2001	8	27*	19:51	−350 nT	19:57	0.25 MA	2.35 A/m	65.45°	34 km	6.4
2001	9	30	19:24	−320 nT	19:27	0.25 MA	1.79 A/m	61.95°	43 km	5
2001	11	6	01:51	−1,210 nT	01:55	(0.84 MA)	(4.74 A/m)	60.70°	(56 km)	4.6
2001	11	19	18:14	−230 nT	18:20	0.24 MA	0.78 A/m	64.73°	99 km	6
2002	8	18*	18:45	−280 nT	18:51	(0.16 MA)	(1.25 A/m)	67.49°	(42 km)	7.5
2004	1	22	01:36	−680 nT	01:40	0.50 MA	4.10 A/m	67.09°	40 km	7.2
2004	7	26	22:49	−570 nT	22:52	0.50 MA	2.48 A/m	65.78°	64 km	6.5
2004	11	9	18:49	−870 nT	18:52	0.79 MA	3.65 A/m	61.70°	70 km	4.9
2005	9	11	01:13	−1,260 nT	01:16	1.25 MA	4.51 A/m	63.62°	88 km	5.6
2012	11	12	23:11	−340 nT	23:17	0.36 MA	1.53 A/m	64.19°	101 km	5.8
2012	11	23*	21:52	−390 nT	21:58	0.42 MA	1.28 A/m	64.94°	103 km	6.1
2013	10	2*	01:55	−520 nT	02:00	0.60 MA	1.66 A/m	65.47°	113 km	6.4
2013	10	8*	20:20	−780 nT	20:30	1.10 MA	2.05 A/m	66.32°	174 km	6.8
2015	6	22	18:33	−590 nT	18:39	0.51 MA	2.53 A/m	64.74°	64 km	6
2017	9	7*	23:00	−1,650 nT	23:05	1.31 MA	7.55 A/m	60.81°	55 km	4.6

Note. SC, sudden commencements: UT, Universal Time. The current parameters listed in columns 5–11 are derived by fitting a model to the ground-based observations at the time of peak deflection. The L-value corresponds to the magnetic latitude (Mlat) of the current peak. Events where an asterisk (*) is added to the day number are followed by a substorm.

a rapid field decrease and a substorm onset are marked in the "day" columns of Tables 1 and 2 by an asterisk. The sixth column lists the onset times. In the fifth column the magnetic latitude of the station closest to substorm onset is listed. The activity commonly start at fairly high latitudes, mostly near the station BJN (71.5° MLat). This is typical for substorms during magnetically quiet periods. This impression is confirmed when looking at the magnetic activity prevailing before the SSC. We have considered the Kp value from the period before the 3-hr interval into which the SC falls. From the Kp values listed in the right-side column one sees that only two events are preceded by Kp > 2.7.

One of our questions was, is there a systematic characteristic in solar wind input that supports the initial activity? For answering that we performed a superposed epoch analysis. Of interest for this analysis are the three components of the IMF, the solar wind velocity and density, as well as the derived dynamic pressure. The point in time when the dynamic solar wind pressure started to increase near the bow shock was used as the key time for lining up the events. First, we stacked all the 92 quiet events and calculated the mean variations of all the six quantities. Figure 7a shows in the lower three panels the solar wind velocity, electron density and dynamic pressure. As expected, all three quantities rapidly increase after the key time, $\Delta t = 0$. In the upper three panels the components of the IMF are plotted. Only the strength of IMF By increases at the key time (approximately doubling), while Bx and Bz show no significant change at the event time. It is worth to note, Bz is on average positive (∼1 nT) before the SC and goes negative only 40 min after the key time.

Somewhat different results are obtained for the 31 events with auroral activity directly following the SC. In the lower part of Figure 7b one can see that the mean step size in pressure increase at the key time is significantly larger than for the quiet events (ΔP: 4.5 vs. 2 nPa). Also, the IMF components show different responses to the SC. The IMF By amplitude increases even more at the key time. But more importantly, Bz is on average negative

Table 2
List of Events Where a Substorm Starts Within About Half an Hour After the SC

Year	Month	Day	UT	Mlat onset	Onset time	Preced. Kp
2000	7	26	18:57	66.2	19:26	2.7
2000	10	5	03:25	66	03:29	5.3
2001	3	27*	01:44	66.2	01:52	1
2001	4	18*	00:46	67.4	00:55	2.3
2001	8	27*	19:51	71.5	20:09	2.3
2001	9	25	20:24	71.5	20:35	0.7
2001	10	28	03:18	64.7	03:42	2.7
2002	5	18	20:08	71.5	20:16	1
2002	8	18*	18:45	71.5	18:59	1.7
2002	11	26	21:52	63.5	22:21	2.3
2005	5	7	19:16	71.5	19:37	2
2005	7	10	03:37	71.5	03:44	4
2011	10	24	18:31	71.5	19:06	1
2012	11	23*	21:52	71.5	22:10	1.3
2013	10	2*	01:55	71.5	02:05	2.3
2013	10	8*	20:20	71.5	20:29	1
2014	2	20	03:18	67.3	03:30	1.3
2015	10	24	18:55	71.5	19:18	0.7
2017	9	7*	23:00	66.1	23:18	2.7

Note. SC, sudden commencements: UT, Universal Time. Events where an asterisk (*) is added to the day number are preceded by an intense westward electrojet right after the SC.

(-2 nT) before and goes even more negative after the SC. Both, the amplification of By and the more southward deflection of Bz enhance, at the time of the SC, the reconnection rate of the IMF with the geomagnetic field, which is in favor of higher magnetic activity.

Statistically, the probabilities for a positive or negative IMF Bz are the same. If just the Bz polarity before the SC would be responsible for the subsequent auroral activity, we should have had about 60 active events. A reason for the missing active cases might be that the interaction of a weak pressure front with the prevailing southward IMF Bz is not sufficient to initiate the strong auroral currents right after the SC. An inspection of all the 92 quiet events confirmed our impression. For most of the cases IMF Bz was positive, others come with small negative (-1 nT) Bz, but they are accompanied by weak SC signatures (10–20 nT).

4. Discussion

The various characteristics of SCs have been studied since many decades. Little attention, however, has been paid to the effects on the nightside, in particular at high latitudes. For the first time we present a comprehensive study of auroral activity starting immediately after the passage of an SC.

An important prerequisite for early auroral activity seems to be the negative IMF Bz for a sufficiently long time before the SC arrival. During that time magnetic flux can pile up in the magnetospheric tail. A sudden disturbance, such as a pressure pulse can initiate a substorm when conditions are favorable (see Lyons et al., 2005). In our collection of active events we have 19 clear cases of substorm initiation within about 30 min after the SC. This is a reasonable time span for the signal to travel from the near-Earth merging site to the ionosphere. Two such events are presented in Figures 4 and 5. Quite common is that many of the substorms start at fairly high latitudes, near the station BJN (71.5° MLat), as is shown in Table 2, fifth column. We have picked the station with the steepest field decrease at the beginning for defining the onset latitude. It has to be noted that BJN is on an island in the middle between Svalbard and Scandinavia with sparse station coverage around. That may explains partly the great number of hits for BJN. The fairly high latitude of substorm onset can be seen as indication for low magnetic activity preceding the substorm. This suggestion is confirmed by the magnetic activity prevailing in the 3-hr interval before the Kp interval into which the SC falls. The right-side column of Table 2 lists these Kp values. They are all below Kp = 3, except for the ones on 5 October 2000 and 10 July 2005. In both cases the SC occurred within a period of magnetic storm time lasting for two days. For the other events we may assume that the tail was not so much stretched and therefore the Earthward accelerated plasma regions were connected to fairly high latitudes. The magnetic flux level in the tail was probably still in an uncritical state, and it needed a sufficiently large magnetic pulse from the SC to start the substorm.

For further confirming the initiation of the substorms we had a look at mid-latitude magnetic field observatories in the same local time sector. Figure 8 depicts conceptually the FACs in the northern and southern hemispheres associated with the substorm current wedge. An intense upward FAC is expected in the pre-midnight sector and the return current should flow somewhere in the morning sector. In addition, the resulting magnetic signatures from the FACs at middle latitudes are also shown for both hemispheres. The northward component, Bx, exhibits positive deflections in both hemispheres, which a peak in the middle between the FAC pairs. Conversely, the eastward, By component goes positive in the vicinity of the upward FAC in the northern hemisphere and negative in the southern hemisphere. These anti-phase variations of the By components at HER, with respect to the northern hemisphere observatories have been used as criteria for identifying the 19 substorm cases listed in Table 2. The By signatures are clearly visible for the examples in Figures 4 and 5.
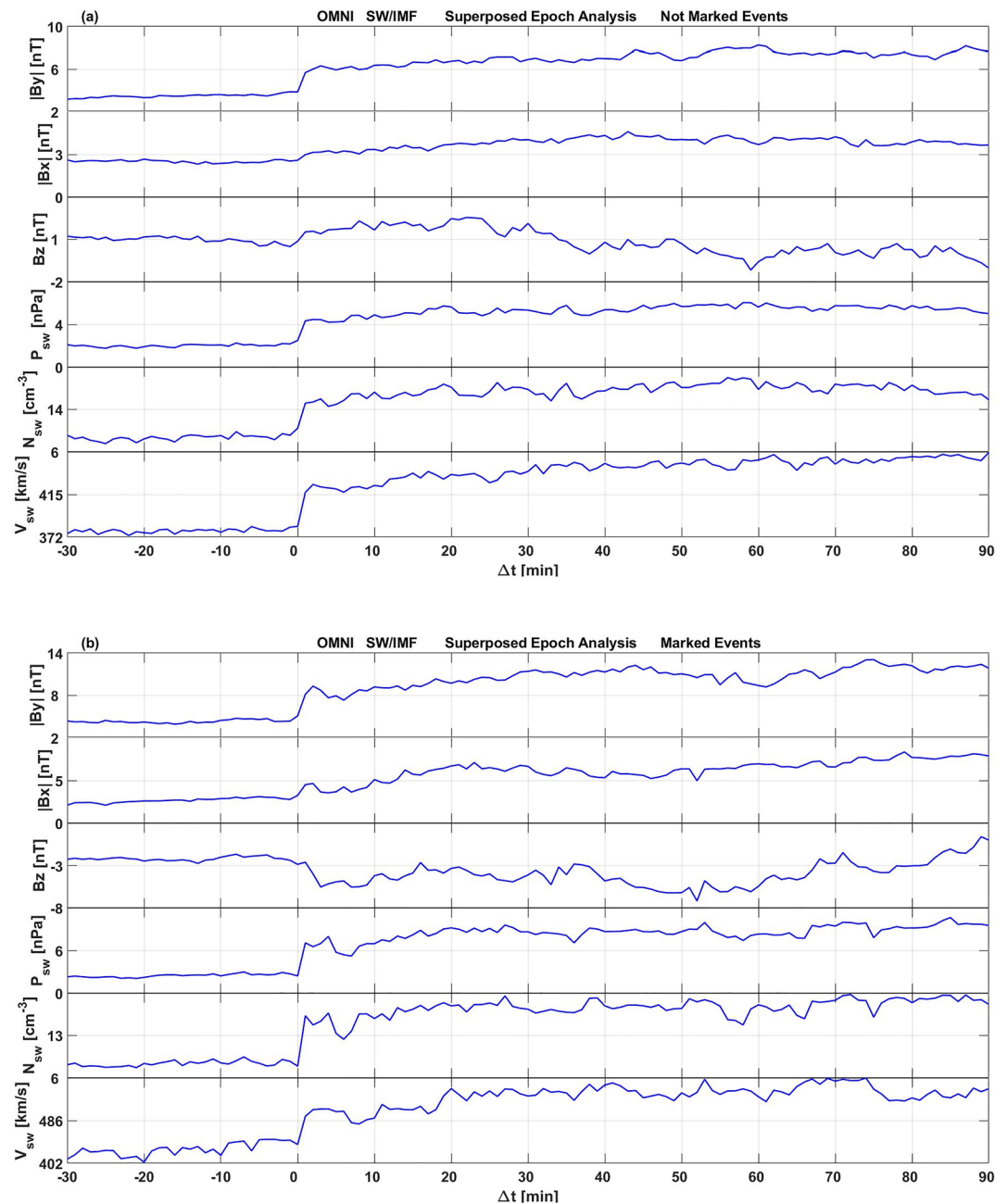
Figure 7. Superposed epoch analysis of interplanetary magnetic field and solar wind parameters around the sudden commencements (SCs); (a) mean evolution of the solar wind and interplanetary magnetic field (IMF) parameters for all the events that were not followed by auroral activity; (b) mean variation of the solar wind input for the events with immediate activity after the SC. At $\Delta t = 0$ the pressure pulse reached the bow shock.

More surprising than the substorms are the intense negative deflections of the X component at auroral latitudes building up only minutes after the SC. These indicate intense westward auroral currents. For a more quantitative characterization of these ionospheric currents, we tried to model their intensity and latitudinal profile from the ground-based observations. Figure 9 shows the latitudinal variations of the X component magnetic deflections for the events presented in Figures 1 and 2. Here the times of peak deflection are presented, which occur in both cases only 3 min after the SC epoch. For estimating the total westward current intensity, we make use of the commonly used virtual line current approach (e.g., Maurer & Theile, 1978)
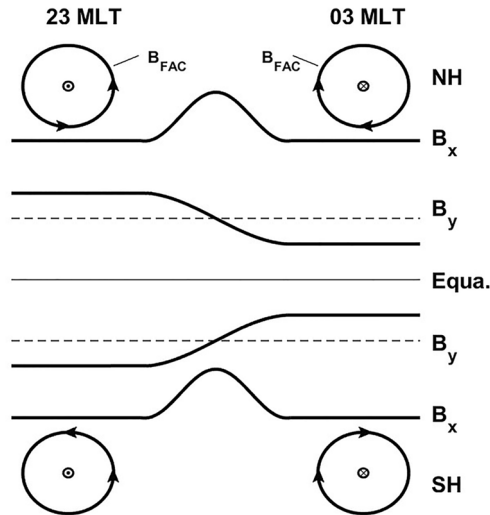
Figure 8. Conceptual illustration of the magnetic deflections caused by the field-aligned currents of a substorm current wedge configuration at middle latitudes in the two hemispheres. Of particular interest is the opposite deflection of the *By* component in the two hemispheres.

$$X = \frac{\mu_0}{2\pi} \frac{I\ (w + h_{\text{ion}})}{(x - x_0)^2 + (w + h_{\text{ion}})^2} \tag{1}$$

where I is the total current, $2w$ is the latitudinal width at half-peak value of the current density, h_{ion} is the height of the ionosphere, here 110 km, x is the position along the latitudinal profile, and x_0 the position of peak deflection. The three unknows: I, w and x_0 have to be determined by fitting the model to the observations at the various sites. As can be seen in Figure 9, a very good agreement between model and observations can be obtained when the following values for the parameters are used.

09-11-2004: $I = -790$ kA, $w = 70$ km, and $x_0 = 61.7°$ MLat.

11-09-2005: $I = -1,250$ kA, $w = 88$ km, and $x_0 = 63.6°$ MLat.

These values show that intense westward currents of order 1 million Ampere are switched on by the SC only minutes after a quiet period.

In a subsequent step we estimated also the latitudinal current density profiles associated with the solutions obtained here. The formula for the height-integrated ionospheric current density, J, corresponding to Equation 1 reads

$$J(x) = \frac{I}{\pi} \frac{(w)}{(x - x_0)^2 + (w)^2} \tag{2}$$

The derived current density profiles for both considered events of westward directed electrojets are shown in Figure 10. It is remarkable to find peak current density values of 3.6 and 4.5 A/m for the first and second event, respectively. Furthermore, the current channel is narrow confined to less than 2° in latitudes in both cases. All this demonstrates the special conditions that are required to drive such intense currents, and these are not the extreme cases. Table 1 lists for comparison the important parameters of the initial electrojets in columns 5–11, peak deflection, peak time, total current, peak current density, peak MLat, half-width, L-value of peak MLat. Many features of the two examples presented before can be found in other cases again. For completeness, we show the fitting of our current model to observations by the IMAGE stations, similar to Figures 9 and 10, for all the 20 events in Supporting Information S1. In cases where no good agreement between model and observations could be achieved the results are presented in Table 1 in parenthesis.

When looking through the current parameters in Table 1, in particular at the half-width of the channel, w, in many cases values around 50 km are obtained. A rule of thumb says, the spatial resolution of ionospheric current systems is comparable to the distance of measurements. In our case, with a typical height of the ionospheric E-layer, reasonable values for w should be of order 50 km or larger. In about half of the studied events we find this limiting value. In reality, however, the intense electrojet could have a much narrower width. An electrojet parameter, rather reliably determined, is the total current value. Since this is independent of the channel width, narrower current strips result in even higher current densities.

Interestingly, we find no particular signatures of these auroral currents in the observations at mid-latitude stations. This may imply a current closer of the electrojet in the ionosphere and no diversion into FACs, as is the cases for substorms. Unfortunately, from ground-based data alone the 3D current distribution cannot be determined. And the region covered by the IMAGE magnetometer network is not even large enough for a 2D picture of equivalent currents, could in our cases indicate the paths of current closure geometry. Simultaneous measurements by LEO satellites could be helpful for clarifying the situation.

A more application-relevant aspect of these intense electrojets after an SC concerns the induction of electric fields in the ground. These will also drive geomagnetically induced currents in power grids and pipelines. The rapid field changes can cause strong (order of 100 A) quasi-DC electric currents in the power lines. Such parasitic currents can have adverse effects in the system (see e.g., Dimmock et al., 2019). As shown above, these disturbances come without warning, appearing out of a quiet background. From the space weather perspective, it may be advisable to watch out for solar wind dynamic pressure jumps in the recording at the Lagrange point, L1. That
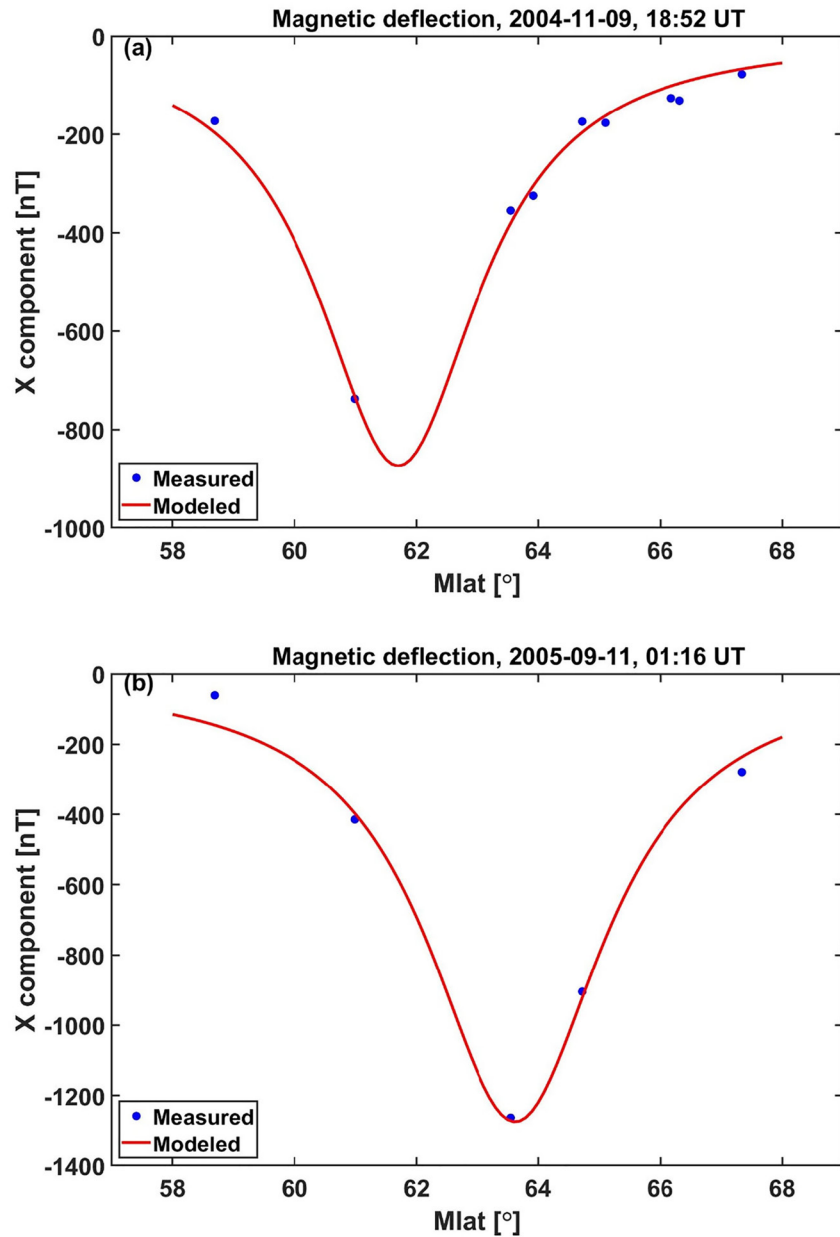
Figure 9. Latitudinal profiles of the magnetic deflections caused by the events shown in Figure 1 (top) and Figure 2 (bottom) at the times of peak current densities. The red curves are derived from an equivalent line current model fitted to the measurements of ground-based stations (blue dots).

provides a warning time of about 1 hour. The conditions favorable for the initiation of a strong electrojet after the SC are outlined above.

In general, it has to be stated that the IMAGE magnetometer data alone are not sufficient to identify the mechanisms in the magnetosphere that drive the intense electrojet right after the SC. Our preferred explanation is that rapid changes in the magnetospheric convection electric field cause kinetic Alfvén waves that propagate along magnetic field lines to the ionosphere at auroral latitudes. These Alfvén waves are accompanied by strong FACs and particle precipitation. A similar event with an intense electrojet preceding a substorm has earlier been described by Lühr et al. (1984) and Klöcker et al. (1985). By employing additional data from other platforms, in
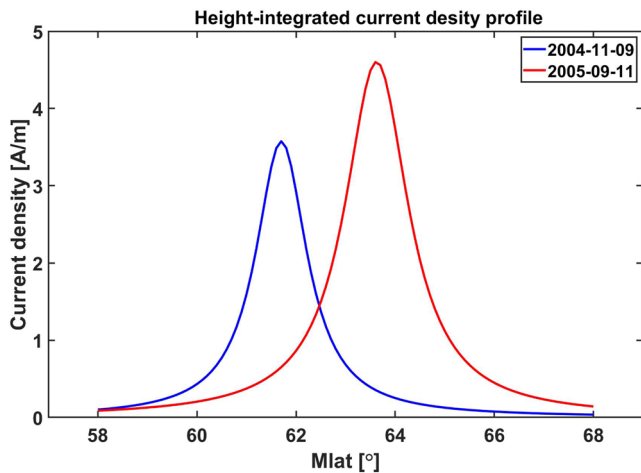
Figure 10. Latitudinal profile of height-integrated ionospheric current densities for the two considered examples, as derived from the fits shown in Figure 9.

space and on ground, we will study the effects in detail and try to confirm in a subsequent paper the suggestions regarding the causes of initial auroral activity after an SC.

5. Summary

In this paper we investigated an aspect of the SC that has not been studied well in the past. Our focus is on the initial and intense electrojet activity immediately following the SC. Based on recordings of the IMAGE Magnetometer Network in Fennoscandia we investigate the partly large negative magnetic deflections peaking only a few minutes after the SC. The main features derived from 21 years of SC detections are summarized below:

1. The variation of SC occurrence frequency over the years follows closely the level of solar activity. Particularly large numbers are detected during the years 2000 and 2001. Another peak occurred at 2014 but reaching only about half the count rates. A surprising observation is an apparent UT-dependence of the SC occurrence rate. Around 24 UT the detection rate reaches only 66% of that at 12 UT. We speculate that this may be caused by the sparse station coverage within the Pacific Ocean region.

2. In a subset of events (about 30%) intense magnetic activity follows directly after the SC. This activity is well confined to auroral latitudes on the nightside. Negative deflections of the order of 1,000 nT reaching peak values on average only 4 min after the SC are not uncommon. These initial disturbances last only some 10 min, and they appear at latitudes magnetically conjugate to region of the nightside magnetosphere at and around geosynchronous distances.

3. In other cases, substorms start after the SC within about 30 min. Their onset occurs at fairly high latitudes ($\sim$71° MLat), and they are preceded by magnetically quiet conditions (Kp < 3). Here the magnetic impulse obviously plays an important role in initiating the substorm. An inspection of mid-latitude magnetograms confirms the signature of the substorm current wedge circuit for these cases. Conversely, the initial negative deflections after the SC exhibit no particular mid-latitude signatures.

4. For determining the role of solar wind input in causing the initial activity after an SC we performed a superposed epoch analysis of the IMF and solar wind parameters. As the key time for stacking the events, the jump in solar wind dynamic pressure was taken. For the active cases we found on average a negative IMF Bz preceding the jump, and it got more negative after it. IMF By increased also significantly at the pressure ramp. Conversely, the SC events not followed by initial activity were preceded by a positive IMF Bz. Furthermore, the step size of the dynamic pressure was on average twice as large for the active cases as for the quiet ones.

From all these observations we may conclude that it requires a preceding negative IMF Bz and an SC with a sufficiently large magnetic pulse to cause the initial auroral activity. The very rapid appearance of the intense disturbance requires particular mechanisms for driving the currents. In a follow-up study we will focus on magnetospheric mechanisms that may cause these initial disturbances after an SC.

Data Availability Statement

The OMNI data are available at http://spdf.gsfc.nasa.gov/pub/data/omni/high_res_omni/.

References

Araki, T. (1977). Global structure of geomagnetic sudden commencements. *Planetary and Space Science*, *25*(4), 373–384. https://doi.org/10.1016/0032-0633(77)90053-8

Araki, T. (1994). A physical model of the geomagnetic sudden commencement. In M. J. Engebretson, K. Takahashi, & M. Scholer (Eds.), *Solar wind sources of magnetospheric ultra-low-frequency waves*. *AGU Geophys. Monograph* (Vol. 81, p. 183).

Chapman, S. (1929). Solar streams of corpuscles: Their geometry, absorption of light and penetration. *Monthly Notices of the Royal Astronomical Society*, *89*, 456–470. https://doi.org/10.1093/mnras/89.5.456

Dimmock, A. P., Rosenqvist, L., Hall, J.-O., Viljanen, A., Yordanova, E., Honkonen, I., et al. (2019). *The GIC and geomagnetic response over Fennoscandia to the 7–8 September 2017 geomagnetic storm* (Vol. 17, pp. 989–1010). Space Weather Space Weather. https://doi.org/10.1029/2018SW002132

Engebretson, M. J., Murr, D. L., Hughes, W. J., Lühr, H., Moretto, T., Posch, J. L., et al. (1999). A multipoint determination of the propagation velocity of a sudden commencement across the polar ionosphere. *Journal of Geophysical Research*, *104*(A10), 22433–22451. https://doi.org/10.1029/1999ja900237

Klöcker, N., Lühr, H., Korth, A., & Robert, P. (1985). Observation of kinetic Alfvén waves excited at substorm onset. *Journal of Geophysics*, *57*(1), 65–71.

Lühr, H., Aylward, A., Bucher, S. C., Pajunpää, A., Pajunpää, K., Holmboe, T., & Zalewski, S. M. (1998). Westward moving dynamic substorm features observed with the IMAGE magnetometer network and other ground-based instruments. In. *Annales Geophysicae*, (Vol, 16, pp. 425–440), Springer-Verlag.

Lühr, H., Klöcker, N., & Thürey, S. (1984). Ground-based observations of a very intense substorm-related pulsation event. *Journal of Geophysics*, *55*, 41–53.

Lühr, H., Schlegel, K., Araki, T., Rother, M., & Förster, M. (2009). Night-time sudden commencements observed by CHAMP and ground-based magnetometers and their relationship to solar wind parameters. In. *Annales Geophysicae*,(Vol, 27, pp. 1897–1907). Retrieved from www.ann-geophys.net/27/1897/2009/

Lyons, L. R., Lee, D. Y., Wang, C. P., & Mende, S. B. (2005). Global auroral responses to abrupt solar wind changes: Dynamic pressure, substorm, and null events. *Journal of Geophysical Research*, *110*(A8), A08208. https://doi.org/10.1029/2005JA011089

Maurer, H., & Theile, B. (1978). Parameters of the auroral electrojet from magnetic variations along a meridian. *Journal of Geophysics*, *44*(1), 415–426.

Petrinec, S. M., Yumoto, K., Lühr, H., Orr, D., Milling, D., Hayashi, K., et al. (1996). The CME event of February 21, 1994: Response of the magnetic field at the Earth's surface. *Journal of Geomagnetism and Geoelectricity*, *48*(11), 1341–1379. https://doi.org/10.5636/jgg.48.1341

Viljanen, A., & Häkkinen, L. (1997). IMAGE magnetometer network. In M. Lockwood, M. N. Wild, & H. J. Opgenoorth (Eds.), *Satellite-Ground Based Coordination Sourcebook* (Vol. 1198, p. 111). Eur. Space Agency Special Publication, ESA-SP.